

# Thermovoltage in quantum dots with attractive interaction

Jens Schulenborg,<sup>1,2</sup> Maarten R. Wegewijs,<sup>3,4,5</sup> and Janine Splettstoesser<sup>2</sup>

<sup>1)</sup>Center for Quantum Devices, Niels Bohr Institute, University of Copenhagen, DK-2100 Copenhagen

<sup>2)</sup>Department of Microtechnology and Nanoscience, Chalmers University of Technology, SE-41298 Göteborg

<sup>3)</sup>Institute for Theory of Statistical Physics, RWTH Aachen, D-52056 Aachen

<sup>4)</sup>JARA- Fundamentals of Future Information Technology

<sup>5)</sup>Peter Grünberg Institut, Forschungszentrum Jülich, D-52425 Jülich

(Dated: 18 May 2022)

We study the linear and nonlinear thermovoltage of a quantum dot with effective *attractive* electron-electron interaction and weak, energy-dependent tunnel-coupling to electronic contacts. Remarkably, we find that the thermovoltage shows signatures of *repulsive* interaction. The characteristics of the thermovoltage get only weakly modified when entering the nonlinear regime of large potential and temperature differences. We expect that the predicted results can be demonstrated in current state-of-the-art experiments. Furthermore, under nonlinear operation, we find extended regions of large power production at efficiencies on the order of the Curzon-Ahlborn bound.

## I. INTRODUCTION

Recently, different types of devices with an effectively attractive electron-electron interaction<sup>1</sup> have been experimentally investigated<sup>2</sup> and also quantum dot structures with attractive onsite-interaction have been realized<sup>3,4</sup>. In these quantum dots, signatures of pair-tunneling<sup>5–7</sup> induced by the attractive onsite interaction could be identified in transport properties.

In the present letter, we predict surprising features in the thermovoltage of such quantum dots. We show that the linear-response thermovoltage — the Seebeck coefficient — shows signatures at quantum-dot level positions that are characteristic for the Coulomb-oscillations due to *repulsive* onsite interaction. This can be exploited for the analysis, in which we show, furthermore, how these features are modified under different, realistic experimental conditions. The discussed effect is highly relevant for the characterization of attractive systems, which has only recently started.

Simultaneously, there has been significant progress in investigating linear and nonlinear-response thermoelectrics in quantum dot devices<sup>8–19</sup>. These are of interest for on-chip energy harvesting and their Seebeck coefficient is a key parameter to characterize them. To our knowledge, our analysis for the first time shows the thermoelectric properties of systems with *strong attractive* electron-electron interaction. We also explicitly address energy-dependent tunnel couplings between dot and environment providing energy filtering in addition to the quantum-dot energy levels. Efficient nanoscale thermoelectrics, in particular three-terminal energy harvesters<sup>10,20–23</sup>, crucially rely on this energy-dependent coupling. In this letter, we characterize the performance of a quantum dot with attractive interaction as steady-state heat engine and find extended regions of large power production and efficiency.

The thermoelectric response of repulsive quantum dots<sup>15,18</sup> has successfully been analyzed using a mapping based on a fermionic duality relation<sup>24</sup>, providing simple analytic formulas. Here, this enables us to explain the full thermoelectric response of a quantum dot with attractive onsite interaction in terms of the well understood physics of a repulsive dot. This simple description can serve as a guide for future experiments.

## II. QUANTUM DOT WITH ATTRACTIVE INTERACTION

We consider a quantum dot, modelled as a single spin-degenerate level, with an *attractive* electron-electron interaction. We assume the level spacing to be large compared to any other energy scale relevant for transport, such as voltage bias and temperatures; indeed, recent experimental realizations of quantum dots with attractive interactions have been well explained in terms of such a model<sup>4</sup>. The isolated dot is then described by the Hamiltonian

$$H = \tilde{\epsilon}N - |U|N_\uparrow N_\downarrow \quad (1)$$

with the single-level energy  $\tilde{\epsilon}$ , the local particle-number operator  $N = N_\uparrow + N_\downarrow$  with spin-resolved components  $N_\uparrow$  and  $N_\downarrow$ , and the interaction strength  $U = -|U|$ . The quantum dot is tunnel-coupled to two electronic reservoirs,  $\alpha = \text{L,R}$ , with electrochemical potentials  $\mu_\text{L} = \mu - V$  and  $\mu_\text{R} = \mu$ , and temperatures  $T_\text{L} = T + \Delta T$  and  $T_\text{R} = T$ . We assume the experimentally relevant case of weak tunnel rates  $\Gamma_\alpha(E) \ll T_\alpha$ , implying that pair-tunneling is enabled by thermal excitations<sup>4,25,26</sup>. We allow these rates to strongly depend on the energy of the tunneling process. We set  $k_\text{B} = \hbar = |e| = 1$ .

We analyze the full thermoelectric response of the quantum dot using expressions obtained from a recently established, general *fermionic duality*<sup>15,18,24,27</sup>. This purely dissipative symmetry, applied to a weak-coupling master-equation description, maps the transport dynamics of fermionic open non-equilibrium systems to those of *dual* systems with sign-inverted local energies, chemical potentials, and energy-dependencies of the tunnel couplings:  $\tilde{\epsilon}, -|U|, \mu_\alpha, \Gamma_\alpha(E) \rightarrow -\tilde{\epsilon}, |U|, -\mu_\alpha, \Gamma_\alpha(-E)$ . In the present case, the remarkable duality enables us to predict *non-equilibrium* effects in the thermoelectric response of the attractive dot of interest by relating them to the properties of the quantum dot with *equilibrium* parameters and attractive interaction as well as to its dual model with *repulsive* interaction<sup>28</sup>. The key quantities in this analysis are the equilibrium dot occupation for attractive interaction

$$n(\epsilon, -|U|) = \langle N \rangle = \frac{2f(\epsilon)}{1 + f(\epsilon) - f(\epsilon - |U|)}, \quad (2)$$

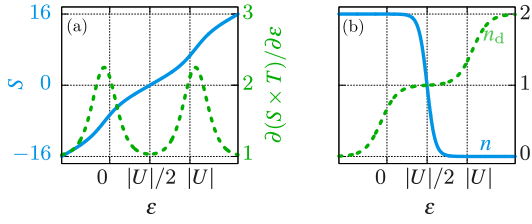


FIG. 1. (a) Seebeck coefficient  $S$  (blue solid) and its derivative (green dashed), and (b) equilibrium charge  $n$  and its dual  $n_d$ , as function of dot level  $\epsilon$ . We take  $T = |U|/10$  and  $\Gamma_{L,R}$  energy-independent.

with  $\epsilon = \tilde{\epsilon} - \mu$  and Fermi function  $f(x) = [\exp(\frac{x}{T}) + 1]^{-1}$ , and most importantly, the *dual* occupation<sup>18</sup>,

$$n_d = n(-\epsilon, |U|) = \frac{2[1-f(\epsilon)]}{1-f(\epsilon)+f(\epsilon-|U|)}, \quad (3)$$

to which the duality assigns a repulsive interaction  $|U|$ . Figure 1(b) shows both  $n$  and  $n_d$  as functions of  $\epsilon$ .

### III. THERMOVOLTAGE

#### A. Seebeck coefficient

We start with the linear response of the thermovoltage, for small  $V$  and  $\Delta T$ , the linear Seebeck coefficient  $S = |V|_{I=0}/\Delta T$ , and first consider energy-independent tunnel couplings  $\Gamma_\alpha(E) \rightarrow \Gamma_\alpha$ . The explicit formula for  $S$  has a remarkably simple form<sup>15</sup> in terms of the dual dot occupation (3),

$$S \times T = \epsilon - |U|(2 - n_d)/2. \quad (4)$$

The consequences of the attractive interaction are shown in Figure 1(a). On the one hand, we find a linear  $\epsilon$ -dependence  $S \times T \approx \epsilon - |U|/2$  around the zero-crossing at  $\epsilon = |U|/2$ . This is intuitively expected in analogy to the well-known case of repulsive quantum dots<sup>15,29-31</sup>: as reflected by  $n(\epsilon)$  in Fig. 1(b), the attractive dot effectively acts as a single resonance at  $\epsilon = |U|/2$ . On the other hand, we find  $S \times T \rightarrow \epsilon - |U|$  for  $\epsilon < 0$  and  $S \times T \rightarrow \epsilon$  for  $\epsilon > |U|$ . Here, the attractive interaction does not anymore favor thermally excited pair transitions over single-electron transitions. The resulting crossovers between all three identified regimes lead to surprising kinks in the Seebeck coefficient  $S(\epsilon)$  [blue line in Fig. 1(a)]. These kinks are even better visible in its derivative<sup>32</sup> [green, dashed line in Fig. 1(a)], measurable using lock-in techniques

$$T \times \frac{\partial S}{\partial \epsilon} = 1 + \delta n_d^2 \times \frac{|U|}{2T}. \quad (5)$$

Indeed, this derivative depends on the equilibrium charge fluctuations  $\delta n_d^2 = \langle N^2 \rangle_d - n_d^2$  after the duality mapping. The latter implies features in  $S(\epsilon)$  at the Coulomb resonances  $\epsilon = 0$  and  $\epsilon = -U = |U|$  of a *repulsive* dot. The occurrence of the dual occupation  $n_d$  in Eq. (4) as the outcome of a brute-force “Fermi’s Gold rule” transport calculation is surprising and defies common physical intuition. This is typical for insights offered by the fermionic duality<sup>15,18,24</sup>.

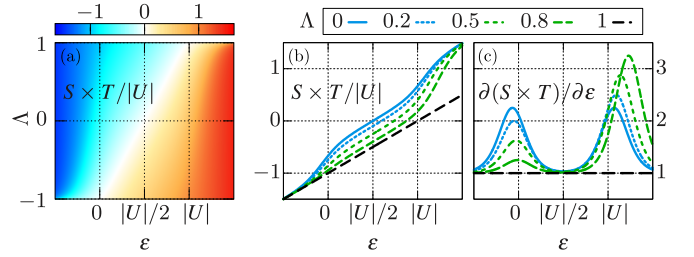


FIG. 2. Seebeck coefficient [(a) and (b)] and its derivative at fixed  $\Lambda$  (c) as function of dot level  $\epsilon$  and coupling-asymmetry  $\Lambda$ . We take energy-dependent  $\Gamma_L(E), \Gamma_R(E)$  and  $T = |U|/10$ .

The mapping to a repulsive system via  $n_d$  enables a further prediction for experiments. The peaks in  $\partial S / \partial \epsilon$  are shifted by approximately  $\pm T \ln(2)$  away from the zero-temperature resonances  $\epsilon = 0, |U|$  of a repulsive dot. In the latter case, this shift is well understood as the entropy of the singly-occupied state due to the spin degeneracy<sup>33-35</sup>. In an attractive dot, single occupation is never a stable equilibrium state, but remarkably, our dual picture reveals that its spin degeneracy nevertheless affects the Seebeck coefficient.

#### B. Influence of energy-dependent coupling

A relevant question is how energy-dependent couplings  $\Gamma_\alpha(E)$  affect the Seebeck coefficient. In experiments, the environment density of states may sizably vary around the Fermi energy and thereby give rise to such an energy dependency. Moreover, an appropriately tuned energy dependence can be beneficial for efficient nanoscale energy harvesting<sup>10,16,20-22</sup>.

We account for this by assuming arbitrary smoothly energy-dependent rates  $\Gamma_{\alpha=L,R}(E) \ll T$  within the weak-coupling constraint. Following Ref. 18,  $S$  is then determined by

$$S \times T = \epsilon - \frac{(1+\Lambda)(2-n_d)}{(1-\Lambda)n_d + (1+\Lambda)(2-n_d)} |U|. \quad (6)$$

This introduces the energy asymmetry  $\Lambda$  of the coupling,

$$\Lambda = \frac{\Gamma_{UL}\Gamma_{UR}\Gamma_\epsilon - \Gamma_{\epsilon L}\Gamma_{\epsilon R}\Gamma_U}{\Gamma_{UL}\Gamma_{UR}\Gamma_\epsilon + \Gamma_{\epsilon L}\Gamma_{\epsilon R}\Gamma_U}, \quad (7)$$

with  $\Gamma_{\epsilon L} = \Gamma_L(\epsilon)$ ,  $\Gamma_{\epsilon R} = \Gamma_R(\epsilon)$ ,  $\Gamma_{UL} = \Gamma_L(\epsilon - |U|)$ ,  $\Gamma_{UR} = \Gamma_R(\epsilon - |U|)$ ,  $\Gamma_\epsilon = \Gamma_{\epsilon L} + \Gamma_{\epsilon R}$ , and  $\Gamma_U = \Gamma_{UL} + \Gamma_{UR}$ . The result for the Seebeck coefficient in the presence of energy-dependent tunnel coupling is shown in Fig. 2. Equation (6) enables us to systematically isolate how energy-dependent couplings  $\Gamma_\alpha(E)$  influence the linear thermovoltage for different level positions  $\epsilon$  at fixed  $U = -|U|$  and  $T$ <sup>36</sup>. In Fig. 2, we identify—as one main qualitative effect of energetic coupling asymmetry—a shift of the zero-crossing of  $S$  as a function of  $\epsilon$  away from  $\epsilon_0 = |U|/2$ . This shift, which we call  $\Delta\epsilon_0$ , can be understood from Eq. (6). We exploit that well within  $0 < \epsilon < |U|$  and for  $|U| \gg T$ , repulsive Coulomb blockade induces a plateau at  $n_d \approx 1$  in the dual occupation. This simplifies Eq. (6) to

$$S \times T \rightarrow \epsilon - (1+\Lambda)|U|/2 \quad \text{for} \quad 0 < \epsilon < |U|, \quad (8)$$

implying that an asymmetry  $\Lambda > 0$  favors emission from a doubly occupied dot at addition energy  $\varepsilon - |U|$ , and an asymmetry  $\Lambda < 0$  favors absorption into an empty dot at energy  $\varepsilon$ . This  $\Lambda$ -dependent offset of  $S(\varepsilon)$  in Eq. (8) involves a zero crossing  $\varepsilon_0$  shifted away from  $|U|/2$  by  $\Delta\varepsilon_0 \rightarrow |U|/2 \times \Lambda$ , predicting a pronounced effect for strong attractive interaction. The limit  $\Delta\varepsilon_0 \rightarrow \pm|U|/2$  for  $\Lambda \rightarrow \pm 1$  reflects that transport is reduced to a single resonance at  $\varepsilon = 0$  or  $\varepsilon = |U|$ , annulling all two-electron features.

Next, Fig. 2(c) demonstrates how the peaks in  $\partial S/\partial\varepsilon$ , and hence the kinks in  $S$  visible in Fig. 1(a), change with energy-dependent couplings. For  $\Lambda > 0$ , the peak in  $\partial S/\partial\varepsilon$  around  $\varepsilon = 0$  shrinks with larger  $|\Lambda|$ , whereas the peak in  $\partial S/\partial\varepsilon$  around  $\varepsilon = |U|$  grows. At the same time, the latter also moves substantially further away from resonance—we refer to this shift from resonance as  $\Delta\varepsilon_p$ . For  $\Lambda < 0$ , the behavior is opposite with respect to the two peaks. In the single-resonance limit  $|\Lambda| \rightarrow 1$ , the slope  $\partial S/\partial\varepsilon \times T \rightarrow 1$  becomes constant and both peaks disappear, as expected.

The change in relative peak height directly follows from the offset of  $S$  within  $0 < \varepsilon < |U|$  described in Eq. (8). For, e.g.,  $\Lambda > 0$ , the shift to smaller  $S$  in this  $\varepsilon$ -interval causes the step of  $S(\varepsilon)$  around  $\varepsilon = 0$  to be smaller than around  $\varepsilon = |U|$ , clearly shown in Fig. 2(b). This results in a smaller relative peak height in  $\partial S/\partial\varepsilon$ .

The growing level shift  $\Delta\varepsilon_p$  of the higher peak for increasing  $|\Lambda|$  stems from the fact that the coupling asymmetry  $\Lambda$  not only affects  $S$  for  $0 < \varepsilon < |U|$  and large  $|U|/T$  as in Eq. (8), but in general influences where the crossover between the single-particle, linear limits [ $S(\varepsilon) \sim \varepsilon$  and  $S(\varepsilon) \sim \varepsilon - |U|$ ] and the two-particle limit [ $S(\varepsilon) \sim \varepsilon - |U|/2$ ] takes place, see Eq. (6). For both small  $|\Lambda|$  and large  $|\Lambda| \lesssim 1$  a useful analytical expression is (including the spin-degeneracy shift  $T \ln(2)$ )

$$\Delta\varepsilon_p \approx T \times \text{sgn}(\Lambda) \times \ln[2/(1 - |\Lambda|)]. \quad (9)$$

For example,  $\Lambda = 0.8$  yields  $\Delta\varepsilon_p \approx 3.3T \ln(2)$ , which substantially deviates from the wideband limit result, where the shift away from resonance is given by  $T \ln(2)$ . In this case,  $\Gamma_U$  is large enough compared to  $\Gamma_\varepsilon$ , such that even for a considerable interval with  $\varepsilon > 0$  and  $\varepsilon - |U| > 0$ , the physics of pair tunneling prevails. Namely, a thermally excited electron entering the dot at energy  $\varepsilon$  causes transport of further electrons at energy  $\varepsilon - |U|$  before the dot is emptied again.

### C. Nonlinear response

Finally, we demonstrate how the Seebeck coefficient gets modified in the nonlinear regime due to large  $\Delta T$  and  $V$ . This is also relevant for Sec. IV discussing the performance of the quantum dot as a thermoelectric device. The nonlinear thermovoltage  $S_{\text{nl}} = V|_{I=0}/\Delta T$  quantifies the voltage  $V = \mu - \mu_L$  required to suppress a charge current  $I$  induced by a large temperature difference  $\Delta T = T_L - T$  across the junction.

We have previously shown<sup>15</sup> the nonlinear current to assume the compact form

$$I = \frac{\gamma_L \gamma_R}{\gamma_L + \gamma_R} (n_L - n_R) \quad (10)$$

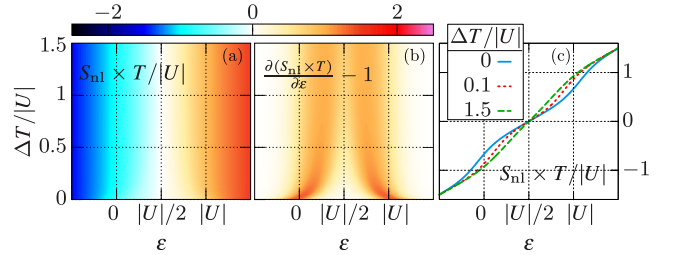


FIG. 3. Nonlinear thermovoltage [(a) and (c)] and its derivative (b) as function of dot level  $\varepsilon$  and temperature gradient  $\Delta T/|U|$ . We take  $T = |U|/10$  and  $\Gamma_L, \Gamma_R$  energy-independent.

in the wideband limit ( $\Gamma_{\varepsilon\alpha} = \Gamma_{U\alpha} = \Gamma_\alpha$ ). This depends on the difference between *equilibrium* occupations  $n_R = n$  and  $n_L = n|_{\mu, T \rightarrow \mu_L, T_L}$ , and on the energy-level dependent charge relaxation rates<sup>37,38</sup>  $\gamma_{R/L} = \Gamma_{R/L} [1 + f_{R/L}(\varepsilon) - f_{R/L}(\varepsilon - |U|)]/2 > 0$ . Both the occupations and relaxation rates can be understood as if the dot was coupled only to the right or left lead; the symbols  $f_R(x) = f(x)$  and  $f_L(x) = f(x)|_{\mu, T \rightarrow \mu_L, T_L}$  denote the corresponding Fermi functions. Setting  $I = 0$  while keeping the potential  $\mu_R = \mu$  and temperature  $T_R = T$  fixed, Eq. (10) yields the analytical result for the thermovoltage<sup>15</sup>

$$S_{\text{nl}} \times T = \varepsilon - |U| \quad (11)$$

$$- \frac{T + \Delta T}{\Delta T/T} \ln \left[ \frac{1 - n_d + \sqrt{(1 - n_d)^2 + e^{-|U|\Delta T}}}{2 - n_d} n_d (2 - n_d) \right]$$

again expressed in terms of the dual occupation number  $n_d$ .

Figure 3 shows  $S_{\text{nl}} \times T$  and its  $\varepsilon$ -derivative<sup>39</sup> as a function of level position  $\varepsilon$  and temperature difference  $\Delta T > 0$ . As expected, the zero crossing at the particle-hole symmetric point  $\varepsilon = |U|/2$  persists. Importantly, the counter intuitive features at  $\varepsilon = 0, |U|$  also continue to exist. This is indeed suggested by Eq. (11), in which the  $\varepsilon$ -dependence enters *entirely* through the dual occupation  $n_d$  determined by repulsive interaction. Specifically, in Fig. 3(c), an increasing  $\Delta T$  transforms the steps at  $\varepsilon = 0, |U|$  between the three regimes of  $S_{\text{nl}}(\varepsilon) \times T$  with equal  $\varepsilon$ -slopes into temperature-broadened transitions between three regimes of *different* slopes. For  $\varepsilon < 0$  and  $\varepsilon > |U|$ ,  $S_{\text{nl}}(\varepsilon) \times T$  still grows with slope 1 as function of  $\varepsilon$ , just as the Seebeck coefficient  $S(\varepsilon) \times T$ , see Fig. 1(a). This again reflects that transport is effectively governed by single-particle physics, see Sec. III B. Within the interval  $0 < \varepsilon < |U|$  in which two-particle effects are relevant, a linear  $\varepsilon$ -dependence of  $S_{\text{nl}} \times T$  with larger slope  $\sim 2$  emerges, as can be qualitatively understood from an analysis of the nonlinear charge current (10): a small  $T \ll |U|$  and a large  $\Delta T \gtrsim |U|$  corresponds to a sharp two-particle transition of  $n_R = 2 \rightarrow 0$ , yet a smooth behavior of  $n_L$  as a function of  $\varepsilon$  around  $\varepsilon = |U|/2$ . Consequently, fulfilling  $n_L = n_R$  to achieve  $I = 0$  for fixed  $\varepsilon$  and  $\mu$  requires a relatively large shift of  $V = \mu - \mu_L$ . In particular, the slope 2 of  $S_{\text{nl}}(\varepsilon) \times T = \frac{VT}{\Delta T}|_{I=0}$  in the limit  $\Delta T/T \gg 1$  reflects the sharp change of  $n_R$  by 2 at  $\varepsilon = |U|/2$ , resulting from attractive interaction, see Fig. 1(b).

#### IV. PERFORMANCE OF POWER PRODUCTION

We conclude our analysis by considering the power output. As well-known<sup>40–43</sup>, a sharp spectral resonance of a conductor is beneficial for its thermoelectric performance. Hence, quantum dots have been studied as thermoelectric elements operated in the nonlinear regime of large temperature and voltage biases, both theoretically<sup>8,9,12,15</sup> and experimentally<sup>11,19</sup>. We now show that also in the presence of strong attractive interaction, finite power output is possible at high efficiencies.

We study the power output  $P = I \times V$  with the current  $I$  given by Eq. (10) as well as the efficiency  $\eta = P/J$ , where  $J$  is the heat current out of the left (hot) reservoir. We use explicit analytical expressions for  $J$ , found in Ref. 15 for a generic onsite interaction. In Fig. 4(a), we show  $P$  and  $\eta$  as function of  $V$  for  $\Delta T = |U|$  and for an  $\varepsilon = 1.23|U|$  in the vicinity of the crossover between single- and two-particle regimes, optimized towards large power output (see below). The power has a clear nonmonotonic behavior with a maximum at  $|V| \approx \Delta T$ . The efficiency  $\eta$  increases with voltage and assumes about 0.6 times the Carnot efficiency  $\eta_C = 1 - T_R/T_L$  at maximum power. That efficiencies are sizable at finite power output can clearly be seen in Fig. 4(b), where efficiency and power are shown for varying voltage (increasing in the direction indicated by the arrow). These also show that efficiencies reach the Carnot limit when power is suppressed at large voltages<sup>44</sup>.

Figures 4(c,d) show the power  $P_{\max}$  maximized over  $V$  at otherwise fixed parameters and the efficiency  $\eta_{P_{\max}}$  at  $P_{\max}$ . Extended regions of  $\varepsilon$ - and  $\Delta T$ -values have sizable power  $P_{\max} \gtrsim \Gamma T$ . Interestingly, Fig. 4(c) shows that the maximum power is fully suppressed only at  $\varepsilon = |U|/2$ . This can be understood by the fact that the nonlinear thermovoltage  $S_{\text{nl}}$  only disappears at this level position, see Sec. III C. However, in the whole two-particle regime,  $0 < \varepsilon < |U|$ , the power is small compared to the single-particle regime,  $\varepsilon < 0$  and  $\varepsilon > |U|$ . The reason is that the charge relaxation rate  $\gamma_R$  entering the current, Eq. (10), is suppressed in this regime by attractive Coulomb blockade<sup>24</sup>. This leads to low power production.

Important for the performance of the attractive quantum dot as a heat engine is that the efficiency at maximum output power is of the order of the Curzon-Ahlborn bound<sup>45</sup>,  $\eta_{\text{CA}} = 1 - \sqrt{T_R/T_L}$ , in the whole range in which the output power is sizable. It even reaches this bound close to the *dual* resonances,  $\varepsilon = 0, |U|$ , namely the level positions at which  $n_d$  obtained from the dual mapping changes by 1. It is remarkable that also for the finite power output, prominent features appear at the resonances of the dual model.

#### V. SUMMARY AND CONCLUSION

We have analyzed the thermoelectric response of a weakly-coupled, single-level quantum dot with attractive interaction together with its performance as a steady-state heat engine. The presented results are expected to be important for future experiments aiming to characterize the physics of attractive onsite interaction. At the same time, they demonstrate that nanodevices based on quantum dots with attractive interac-

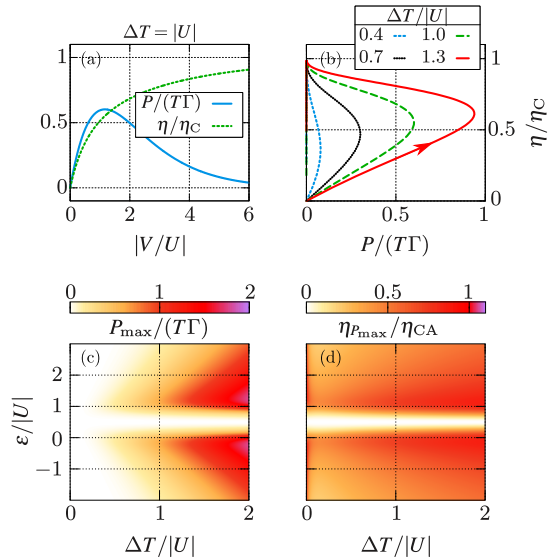


FIG. 4. (a) Power  $P$  and efficiency  $\eta$  as function of the voltage bias  $V$  at fixed level position,  $\varepsilon = 1.23|U|$ ,  $\Delta T = |U|$ ,  $T = |U|/10$ . (b) Efficiency versus power at fixed level position,  $\varepsilon = 1.23|U|$  for different temperature biases  $\Delta T$ . (c) Power  $P_{\max}$  maximized over  $V$ . (d) Efficiency  $\eta_{P_{\max}}$  at maximum power.

tion can efficiently convert heat to work. We anticipate the predicted effects to be visible in state-of-the-art experiments.

The remarkable appearance of prominent features at level positions characteristic for a repulsive quantum dot could be predicted and rationalized using a dual mapping emerging from a dissipative symmetry for master equations. For an attractive quantum dot, the role of the dual mapping turns out to be particularly important: The dual features with respect to the original attractive system *do not* appear at special positions, where e.g. particle-hole symmetry imposes restrictions. Their prominent role could hence not have been predicted straightforwardly in another way.

#### ACKNOWLEDGMENTS

We acknowledge financial support from the Knut and Alice Wallenberg foundation and the Swedish VR (J.Sp., J.Sc.) and the Danish National Research Foundation (J.Sc.).

<sup>1</sup>M. R. Butler, B. Movaghari, T. J. Marks, and M. A. Ratner, “Electron Pairing in Designer Materials: A Novel Strategy for a Negative Effective Hubbard U,” *Nano Lett.* **15**, 1597–1602 (2015).

<sup>2</sup>G. Cheng, M. Tomczyk, S. Lu, J. P. Veazey, M. Huang, P. Irvin, S. Ryu, H. Lee, C.-B. Eom, C. S. Hellberg, and J. Levy, “Electron pairing without superconductivity,” *Nature* **521**, 196 (2015).

<sup>3</sup>A. Hamo, A. Benyaminini, I. Shapir, I. Khivrich, J. Waissman, K. Kaasbjerg, Y. Oreg, F. von Oppen, and S. Ilani, “Electron attraction mediated by Coulomb repulsion,” *Nature* **535**, 395 (2016).

<sup>4</sup>G. E. D. K. Prawiroatmodjo, M. Leijnse, F. Trier, Y. Chen, D. V. Christensen, M. von Soosten, N. Pryds, and T. S. Jespersen, “Transport and excitations in a negative-U quantum dot at the LaAlO<sub>3</sub>/SrTiO<sub>3</sub> interface,” *Nat. Commun.* **8**, 395 (2017).

<sup>5</sup>J. Koch, M. E. Raikh, and F. von Oppen, “Pair Tunneling through Single Molecules,” *Phys. Rev. Lett.* **96**, 056803 (2006).

<sup>6</sup>E. Sela, H.-S. Sim, Y. Oreg, M. E. Raikh, and F. von Oppen, “Electron-Pair Resonance in the Coulomb Blockade,” *Phys. Rev. Lett.* **100**, 056809 (2008).

<sup>7</sup>M. Leijnse, M. R. Wegewijs, and M. H. Hettler, “Pair Tunneling Resonance in the Single-Electron Transport Regime,” *Phys. Rev. Lett.* **103**, 156803 (2009).

<sup>8</sup>M. Esposito, K. Lindenberg, and C. Van den Broeck, “Thermoelectric efficiency at maximum power in a quantum dot,” *EPL* **85**, 60010 (2009).

<sup>9</sup>M. Leijnse, M. R. Wegewijs, and K. Flensberg, “Nonlinear thermoelectric properties of molecular junctions with vibrational coupling,” *Phys. Rev. B* **82**, 045412 (2010).

<sup>10</sup>R. Sánchez and M. Büttiker, “Optimal energy quanta to current conversion,” *Phys. Rev. B* **83**, 085428 (2011).

<sup>11</sup>S. F. Svensson, E. A. Hoffmann, N. Nakpathomkun, P. M. Wu, H. Q. Xu, H. A. Nilsson, D. Sánchez, V. Kashcheyevs, and H. Linke, “Nonlinear thermovoltage and thermocurrent in quantum dots,” *New J. Phys.* **15**, 105011 (2013).

<sup>12</sup>D. M. Kennes, D. Schuricht, and V. Meden, “Efficiency and power of a thermoelectric quantum dot device,” *EPL* **102**, 57003 (2013).

<sup>13</sup>B. Sothmann, R. Sánchez, and A. N. Jordan, “Thermoelectric energy harvesting with quantum dots,” *Nanotechnology* **26**, 032001 (2014).

<sup>14</sup>A. Svilans, A. M. Burke, S. F. Svensson, M. Leijnse, and H. Linke, “Nonlinear thermoelectric response due to energy-dependent transport properties of a quantum dot,” *Physica E* **82**, 34–38 (2016).

<sup>15</sup>J. Schulenborg, A. Di Marco, J. Vanherck, M. R. Wegewijs, and J. Splettstoesser, “Thermoelectrics of Interacting Nanosystems—Exploiting Superselection Instead of Time-Reversal Symmetry,” *Entropy* **19**, 668 (2017).

<sup>16</sup>N. Walldorf, A.-P. Jauho, and K. Kaasbjerg, “Thermoelectrics in Coulomb-coupled quantum dots: Cotunneling and energy-dependent lead couplings,” *Phys. Rev. B* **96**, 115415 (2017).

<sup>17</sup>P. A. Erdman, F. Mazza, R. Bosisio, G. Benenti, R. Fazio, and F. Taddei, “Thermoelectric properties of an interacting quantum dot based heat engine,” *Phys. Rev. B* **95**, 245432 (2017).

<sup>18</sup>J. Schulenborg, J. Splettstoesser, and M. R. Wegewijs, “Duality for open fermion systems: Energy-dependent weak coupling and quantum master equations,” *Phys. Rev. B* **98**, 235405 (2018).

<sup>19</sup>M. Josefsson, A. Svilans, A. M. Burke, E. A. Hoffmann, S. Fahlvik, C. Thelander, M. Leijnse, and H. Linke, “A quantum-dot heat engine operating close to the thermodynamic efficiency limits,” *Nat. Nanotechnol.* **13**, 920–924 (2018).

<sup>20</sup>F. Hartmann, P. Pfeffer, S. Höfling, M. Kamp, and L. Worschech, “Voltage Fluctuation to Current Converter with Coulomb-Coupled Quantum Dots,” *Phys. Rev. Lett.* **114**, 146805 (2015).

<sup>21</sup>B. Roche, P. Roulleau, T. Jullien, Y. Jompol, I. Farrer, D. A. Ritchie, and D. C. Glattli, “Harvesting dissipated energy with a mesoscopic ratchet,” *Nat. Commun.* **6**, 6738 (2015).

<sup>22</sup>H. Thierschmann, R. Sánchez, B. Sothmann, F. Arnold, C. Heyn, W. Hansen, H. Buhmann, and L. W. Molenkamp, “Three-terminal energy harvester with coupled quantum dots,” *Nat. Nanotechnol.* **10**, 854 (2015).

<sup>23</sup>H. Thierschmann, R. Sánchez, B. Sothmann, H. Buhmann, and L. W. Molenkamp, “Thermoelectrics with Coulomb-coupled quantum dots,” *C.R. Phys.* **17**, 1109–1122 (2016).

<sup>24</sup>J. Schulenborg, R. B. Saptsov, F. Haupt, J. Splettstoesser, and M. R. Wegewijs, “Fermion-parity duality and energy relaxation in interacting open systems,” *Phys. Rev. B* **93**, 081411 (2016).

<sup>25</sup>E. Kleinherbers, P. Stegmann, and J. König, “Revealing attractive electron-electron interaction in a quantum dot by full counting statistics,” *New J. Phys.* **20**, 073023 (2018).

<sup>26</sup>B. A. Placke, T. Pluecker, J. Splettstoesser, and M. R. Wegewijs, “Attractive and driven interactions in quantum dots: Mechanisms for geometric pumping,” *Phys. Rev. B* **98**, 085307 (2018).

<sup>27</sup>V. Bruch, K. Nestmann, J. Schulenborg, and M. R. Wegewijs, (2020), in preparation.

<sup>28</sup>Up to linear order in the couplings  $\Gamma_\alpha$ , the dual model is a physically valid model and can be interpreted physically. This breaks down in higher-than-linear orders in  $\Gamma_\alpha$ , but the duality remains useful<sup>27</sup>.

<sup>29</sup>C. W. J. Beenakker and A. A. M. Staring, “Theory of the thermopower of a quantum dot,” *Phys. Rev. B* **46**, 9667 (1992).

<sup>30</sup>A. A. M. Staring, L. W. Molenkamp, B. W. Alphenaar, H. van Houten, O. J. A. Buyk, M. A. A. Mabesoone, C. W. J. Beenakker, and C. T. Foxon, “Coulomb-Blockade Oscillations in the Thermopower of a Quantum Dot,” *EPL* **22**, 57 (1993).

<sup>31</sup>A. S. Dzurak, C. G. Smith, M. Pepper, D. A. Ritchie, J. E. F. Frost, G. A. C. Jones, and D. G. Hasko, “Observation of Coulomb blockade oscillations in the thermopower of a quantum dot,” *Solid State Commun.* **87**, 1145–1149 (1993).

<sup>32</sup>The relation  $\delta n_d^2 = T \partial n_d / \partial \epsilon$  is proven in Ref. 15.

<sup>33</sup>M. M. Deshmukh, E. Bonet, A. N. Pasupathy, and D. C. Ralph, “Equilibrium and nonequilibrium electron tunneling via discrete quantum states,” *Phys. Rev. B* **65**, 073301 (2002).

<sup>34</sup>E. Bonet, M. M. Deshmukh, and D. C. Ralph, “Solving rate equations for electron tunneling via discrete quantum states,” *Phys. Rev. B* **65**, 045317 (2002).

<sup>35</sup>S. Juergens, F. Haupt, M. Moskalets, and J. Splettstoesser, “Thermoelectric performance of a driven double quantum dot,” *Phys. Rev. B* **87**, 245423 (2013).

<sup>36</sup> $\Lambda$  actually depends on  $\epsilon$  via  $\Gamma_\alpha(E)$  [Eq. (7)]. In Fig. 2,  $\epsilon$  is swept while adjusting  $\Gamma_\alpha(E)$  to keep  $\Lambda$  constant. However, as Ref. 18 has shown, an  $\epsilon$ -sweep that keeps  $\Lambda$  constant is achieved without adjusting the couplings for an exponential  $\Gamma_\alpha(E) \sim \exp((E - E_0)/D)$ . Such an energy-profile has proven to be a reasonable assumption in analyzing several past experiments on few-electron transport from quantum dots.<sup>46–49</sup>

<sup>37</sup>J. Splettstoesser, M. Governale, J. König, and M. Büttiker, “Charge and spin dynamics in interacting quantum dots,” *Phys. Rev. B* **81**, 165318 (2010).

<sup>38</sup>J. Vanherck, J. Schulenborg, R. B. Saptsov, J. Splettstoesser, and M. R. Wegewijs, “Relaxation of quantum dots in a magnetic field at finite bias – Charge, spin, and heat currents,” *Phys. Status Solidi B* **254**, 1600614 (2017).

<sup>39</sup>The derivative can be straightforwardly analytically obtained from Eq. (11).

<sup>40</sup>G. D. Mahan and J. O. Sofo, “The best thermoelectric,” *Proc. Natl. Acad. Sci. U.S.A.* **93**, 7436–7439 (1996).

<sup>41</sup>L. D. Hicks and M. S. Dresselhaus, “Effect of quantum-well structures on the thermoelectric figure of merit,” *Phys. Rev. B* **47**, 12727–12731 (1993).

<sup>42</sup>L. D. Hicks and M. S. Dresselhaus, “Thermoelectric figure of merit of a one-dimensional conductor,” *Phys. Rev. B* **47**, 16631(R)–16634 (1993).

<sup>43</sup>T. E. Humphrey and H. Linke, “Reversible Thermoelectric Nanomaterials,” *Phys. Rev. Lett.* **94**, 096601 (2005).

<sup>44</sup>The sharp feature at low power and high efficiencies stems from the exponential tails of  $n_{LR}$  prohibiting an exactly suppressed current. We expect this to be smoothed by here neglected higher-order tunneling effects.

<sup>45</sup>F. L. Curzon and B. Ahlborn, “Efficiency of a Carnot engine at maximum power output,” *Am. J. Phys.* **43**, 22 (1998).

<sup>46</sup>K. A. Matveev and L. I. Glazman, “Coulomb blockade of activated conduction,” *Phys. Rev. B* **54**, 10339–10341 (1996).

<sup>47</sup>N. M. Zimmerman, E. Houdakis, Y. Ono, A. Fujiwara, and Y. Takahashi, “Error mechanisms and rates in tunable-barrier single-electron turnstiles and charge-coupled devices,” *J. Appl. Phys.* **96**, 5254–5266 (2004).

<sup>48</sup>J. D. Fletcher, M. Kataoka, S. P. Giblin, S. Park, H.-S. Sim, P. See, D. A. Ritchie, J. P. Griffiths, G. A. C. Jones, H. E. Beere, and T. J. B. M. Janssen, “Stabilization of single-electron pumps by high magnetic fields,” *Phys. Rev. B* **86**, 155311 (2012).

<sup>49</sup>B. Kaestner and V. Kashcheyevs, “Non-adiabatic quantized charge pumping with tunable-barrier quantum dots: a review of current progress,” *Rep. Prog. Phys.* **78**, 103901 (2015).